Check for updates

Received: 30 May 2023 | Revised: 2 October 2023 | Accepted: 24 October 2023

DOI: 10.1002/mawe.202300141

ARTICLE

WILEY VCH

Analysis of response signals to minimally invasive laser modulation in laser cutting

Analyse der Antwortsignale auf minimalinvasive Lasermodulation beim Laserstrahlschneiden

M. de Oliveira Lopes[1] | **F. Schneider**[2] | **D. Petring**[2] | **A. Gillner**[1, 2]

[1]RWTH Aachen University, Chair for Laser Technology LLT, Aachen, Germany

[2]Fraunhofer Institute for Laser Technology ILT, Aachen, Germany

Correspondence
M. de Oliveira Lopes, RWTH Aachen University, Chair for Laser Technology LLT, 52074 Aachen, Germany.
Email: marcelo.lopes@llt.rwth-aachen.de

Abstract

A robust real-time monitoring system for the laser cutting process has been targeted by researchers and users for several decades without significant breakthrough. The use of coaxial photodiodes provides a cost-effective and straightforward system; however, the assessment of the process state based on the spatially integrated detected signals can lead to misinterpretation due to the numerous and interacting parameter dependencies of the signals. To obtain a clear correlation of the signals to the process state, minimally invasive laser modulation stimulates characteristic state-dependent response signals. In this study, the response signals to a laser power modulation are analyzed in the visible and infrared range. Furthermore, a spatially and temporally resolved analysis of the process response is enabled by means of high-speed videography. This provides a comprehensive understanding of the process state in terms of temperature and geometry response to the modulation and offers a reliable exploitation of process emissions for real-time monitoring and control applications.

KEYWORDS
high-speed videography, laser cutting, laser modulation, photodiode, process monitoring

Abstract

Ein robustes Echtzeit-Überwachungssystem für den Laserstrahlschneidprozess wird von Forschern und Anwendern seit mehreren Jahrzehnten angestrebt, ohne dass ein signifikanter Durchbruch erzielt wurde. Die Verwendung von koaxialen Photodioden bietet ein kosteneffizientes und unkompliziertes System; die Identifizierung des Prozesszustands auf Basis der räumlich integrierten detektierten Signale kann jedoch aufgrund der zahlreichen und wechselwirkenden Parameterabhängigkeiten der Signalanteile zu Fehlinterpretationen führen. Um eine eindeutige Korrelation der Signale zum Prozesszustand zu erhalten, stimuliert

This is an open access article under the terms of the Creative Commons Attribution Non-Commercial NoDerivs License, which permits use and distribution in any medium, provided the original work is properly cited, the use is non-commercial and no modifications or adaptations are made.
© 2024 The Authors. *Materialwiss. Werkstofftech.* published by Wiley-VCH GmbH.

die minimalinvasive Lasermodulation charakteristische zustandsabhängige Antwortsignale. In dieser Studie werden die Antwortsignale auf eine Laserleistungsmodulation im sichtbaren und infraroten Bereich analysiert. Darüber hinaus wird eine räumlich und zeitlich aufgelöste Analyse der Prozessantwort mittels Highspeed-Videografie ermöglicht. Dies liefert ein umfassendes Verständnis des Prozesszustands in Bezug auf die Temperatur- und Geometrieantwort auf die Modulation und bietet eine zuverlässige Ausnutzung von Prozessemissionen für Echtzeit-Überwachungs- und Regelungsanwendungen.

SCHLÜSSELWÖRTER
Highspeed-Videografie, Lasermodulation, Laserstrahlschneiden, Photodiode, Prozessüberwachung

1 | INTRODUCTION

Laser cutting is an established industrial process and has been the world's largest market in the laser industry over the past years [1]. Nevertheless, good cut surface quality can only be achieved within a narrow range of parameters especially in laser cutting of metal sheets in the medium and thick ranges [2]. Not only operator error in parameter settings and system adjustment, but optics contamination and thermal effects can push the process out of this range, resulting in deterioration of the cut or even an incomplete cut. A real-time monitoring and control system is the logical approach towards addressing this issue. As early as in the 1980s, scientific studies have been conducted to develop a process monitoring system for laser cutting, with one of the first approaches being to monitor the shower of sparks underneath the sheet during cutting [3,4]. Later many studies have opted for a coaxial photodiode-based monitoring system [5,6]. Several advantages favor the use of coaxial photodiodes for industrial applications, such as the low price, the easy integration into existing beam paths, and the detection of process signals independent of the cutting direction. Both geometry and temperature changes of the cutting front are detected with this method [7,8]. The detector signal increases when the surface temperature is increased. In addition, the change in geometry of the cutting front has an impact on the signal level by the size of the projection in the direction of the laser beam axis. Flattening of the cutting front leads to an increase in the detector signal due to the increase in the area projected in the detector plane. Amongst others, due to these mixed effects assessing the process state based solely on the signal level can lead to misinterpretations. For instance, the modification of the arrangement between nozzle and kerf (e.g., stand-off distance, beam misalignment) or a change of the focus position can greatly change the light intensity detected by the photodiodes, even if the cutting front geometry and the process temperature are not significantly altered. Therefore, a method for increasing the signal significance in a coaxial photodiode-based monitoring system that allows reliable exploitation of process emissions during laser cutting is to be developed.

2 | MINIMALLY INVASIVE LASER MODULATION

The utilization of minimally invasive laser modulation draws on earlier investigations of the laser cutting process response on laser power modulation [7,8] and its basics have been published so far only one time and nearly two decades ago [9]. The fundamental principle of the approach is based on the state-dependent response of the cutting front to a moderate temporal modulation of the laser power (e.g., 20%) in the form of a square wave power reduction. A stable process exhibits a fast temperature decrease due to the sudden reduction of power followed by a movement of the colder cutting front into the interaction zone due to the continued movement of the laser spot and a steep rise of temperature when power returns to the original level, Figure 1 [9]. This leads to a characteristic peak in the signal. After that, the process regains its original steady state level. The related change in the process signal signature provides valuable information for process monitoring and control [9].

To utilize the available laser power and minimize the effects of laser modulation on the cutting process, ideally the lower laser power level is short and high enough to avoid a significant disturbance of the cutting process. This results in an asymmetric modulation pattern with a short and moderate reduction of the laser power, which nevertheless stimulate characteristic, state-dependent signals without reducing the cut flank quality.

15214052, 2024, 1, Downloaded from https://onlinelibrary.wiley.com/doi/10.1002/mawe.202300141 by Rwth Aachen Hochschulbibliothek, Wiley Online Library on [15/05/2024]. See the Terms and Conditions (https://onlinelibrary.wiley.com/terms-and-conditions) on Wiley Online Library for rules of use; OA articles are governed by the applicable Creative Commons License

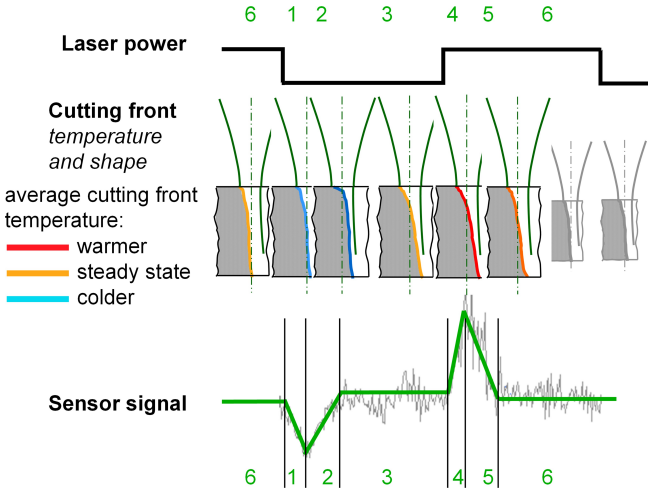

FIGURE 1 The idealized response signal of a stable process to a temporal laser modulation with a square wave signal form and a sketch indicating the temperature and shape of the cutting front; Reproduced with permission [8].

3 | AIM OF THE INVESTIGATION

High-speed videography is used to provide a spatially and temporally resolved in-depth analysis of the process response to minimally invasive laser modulation. This investigation supports the optimization of a monitoring and control system based on this laser modulation approach.

4 | MATERIALS AND EXPERIMENTAL DETAILS

The experiments were performed using a disk laser with a wavelength of 1030 nm and a maximum output power of 6 kW. A Precitec HPSSL cutting head was used, and the fiber-guided laser beam (Ø = 100 µm) was collimated and focused with focal lengths of 100 mm and 200 mm, respectively. This configuration results in a focal diameter of 200 µm. A standard conical nozzle with a diameter of 3 mm at a stand-off distance of 0.7 mm was used. The nitrogen gas pressure was 18 bar to cut 6 mm thick stainless-steel samples with a cutting speed of 4.0 m min^{-1}, which corresponds to about 80 % of the cutting speed limit and ensures a stable process with good cut flank quality, characterized by an average surface roughness inferior than 40 µm and a maximum burr length below 80 µm. The focus was set 3 mm below the sheet surface yielding a kerf with average width of 400 µm. The laser power was modulated from its maximum output power of 6.0 kW (100 %) to 3.6 kW (60 %) or 4.8 kW (80 %). The duration of the modulation period was maintained constant at 3 ms, and the duration of the laser power at the lower level was 0.1, 0.2 and 0.5 ms, Table 1. In addition, a cut with constant laser power of 6 kW was analyzed as a reference.

The monitoring system is based on the acquisition of the thermal emissions of the cutting front by means of photodiodes (LCM sensor, Precitec KG). During the cutting process, thermal radiation is emitted from the cutting front according to its geometry and temperature which can be used to identify the process state. Part of the radiation enters the cutting nozzle concentrically arranged to the beam through the nozzle opening, passes the focusing lens and hits two photodiodes, one for the visible (VIS) and one for the infrared (IR) wavelength range. The detectors convert the radiation power according to their sensitivity into a photocurrent being turned into a proportional voltage signal (0–10 V) via a subsequent operational amplifier. An appropriate amplification level was selected. The signals were recorded by means of a data acquisition card with a sample rate of 200 kHz. A high-speed camera (Photron SA 5) was employed to perform a spatially and temporally resolved diagnosis of the process response on the cutting front. Its direction of observation was aligned through the developing kerf horizontally in cutting direction, Figure 2. The frame rate in the videos was set to 162750 frames per second and a spatial resolution of 21 µm/px was enabled by using a macro lens with a focal length of 200 mm. The generated images have a resolution of 28 px×280 px (0.6 mm×6.0 mm) and show a centered

TABLE 1 Main process parameters in the cutting experiments.

Fixed parameter	Unit	Value
Material	–	1.4301
Sheet thickness	[mm]	6.0
Laser power (100 %) – P_{high}	[kW]	6.0
Cutting speed – v	[m min^{-1}]	4.0
Fiber diameter	[µm]	100
Focal length collimator	[mm]	100
Focal length focussing optics	[mm]	200
Focal position	[mm]	−3.0
Gas pressure (N_2)	[bar]	18
Stand-off distance	[mm]	0.7
Nozzle diameter	[mm]	3.0
Varied parameters	**Unit**	**Value**
Laser power at the lower level – P_{low}	[kW]	4.8, 3.6
Duration of laser power at the lower level – t_{low}	[ms]	0.1, 0.2, 0.5

15214052, 2024, 1, Downloaded from https://onlinelibrary.wiley.com/doi/10.1002/mawe.202300141 by Rwth Aachen Hochschulbibliothek, Wiley Online Library on [15/05/2024]. See the Terms and Conditions (https://onlinelibrary.wiley.com/terms-and-conditions) on Wiley Online Library for rules of use; OA articles are governed by the applicable Creative Commons License

cutting front. Moreover, a short-pass filter was used to filter out emissions with a wavelength above 1000 nm and the associated reflections of the laser beam, such that primarily the thermal emissions from the cutting front were detected. In addition to the evaluation of the individual images of the cutting front, the method of streak imaging of the cutting front apex was adopted, which has previously proven to be a valuable tool for analyzing the dynamics of the melt waves sliding down on the cutting front [10].

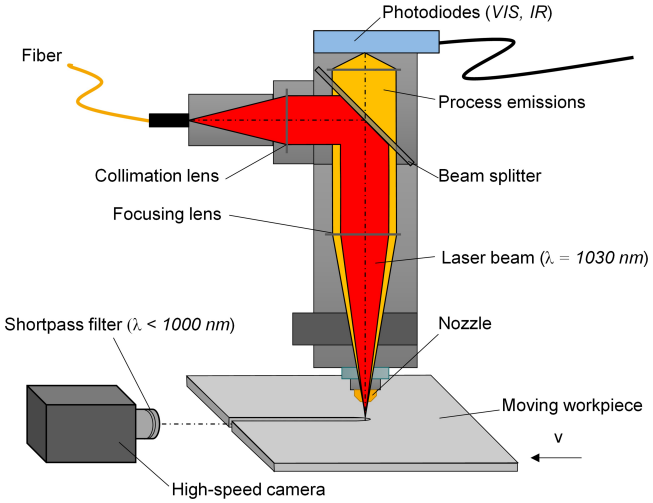

FIGURE 2 Sketch of the experimental setup.

5 | RESULTS AND DISCUSSION

The photodiode signals acquired during the reference cut with constant laser power of 6 kW show typical stochastic behavior, Figure 3. Compared to the infrared (IR)-signal, the visible (VIS)-signal has a lower mean value (0.85 V versus 1.19 V) but a larger variation (0.14 V versus 0.06 V), suggesting that it is more responsive to process dynamics under these conditions.

The application of minimally invasive laser modulation generates valleys in the signals in response to the reduction of the laser power. A reduction to 4.8 kW and for short durations result in a weak process response being hidden in the standard signal variation.

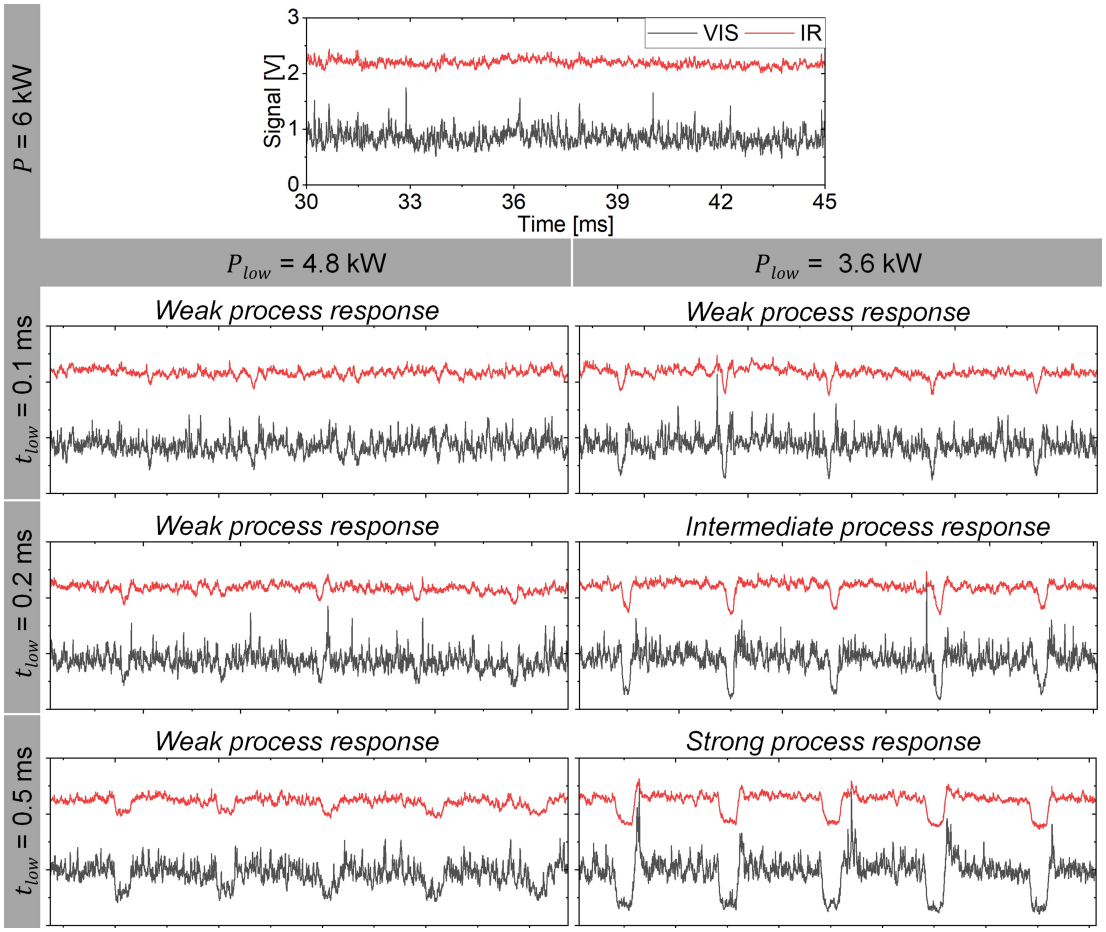

FIGURE 3 Overview of the photodiode signals; signal from the emissions in the infrared range raised by one volt for better visualization.

15214052, 2024, 1, Downloaded from https://onlinelibrary.wiley.com/doi/10.1002/mawe.202300141 by Rwth Aachen Hochschulbibliothek, Wiley Online Library on [15/05/2024]. See the Terms and Conditions (https://onlinelibrary.wiley.com/terms-and-conditions) on Wiley Online Library for rules of use; OA articles are governed by the applicable Creative Commons License

Furthermore, the characteristic maximum peak after increasing the laser power cannot be identified. The reduction of the laser power to 3.6 kW clearly has a greater effect on the signals. The valleys in the signals stand out from the steady state condition, and with increasing the duration of the laser power at the lower level, the height of the characteristic peak increases.

The process response is analyzed in greater depth using streak patterns which appear as process response in the streak images of the cutting front apex extracted from the high-speed videos. The streak patterns can be interpreted more easily by averaging over in this case 12 modulation periods of the streak recordings. From this, spatially and temporally resolved diagnostic information about the process response can be derived. The y-axis defines the spatial domain to be analyzed, namely the cutting front apex, and the x-axis indicates the temporal evolution of the melt waves sliding downstream. Accordingly, the inclination of the steeper and narrow white stripes reveals the downward velocity of the melt waves, and the gray value correlates with the temperature.

The streak pattern of the reference cut is characterized by a gradual increase in the brightness of the white stripes with the cutting depth, indicating an increase of temperature towards the lower part of the cutting front, whereas the dark areas with lower periodicity and inclination represent cold areas or even torn parts of the melt film between melt accumulations moving down with slower speed [11], Figure 4.

The use of minimally invasive laser modulation results in a dark zone on the left-hand side in the streak patterns, caused by the cooling of the cutting front due to the reduction of the laser power. It is more prominent in the case of $P_{low} = 3.6$ kW, illustrating the obvious greater decrease of temperature in this case. The colder zone presents a discontinuous progression in space and time, especially in the upper third section. This effect becomes more pronounced by increasing t_{low}. This is attributed to the reshaping and shifting of the cutting front towards the laser beam axis as a result of the cooling and the related reduced material removal rate at the lower power level. Given the Gaussian-like profile of the laser beam, the radiation is more intense near the laser beam axis. Accordingly, during the reshaping process the cutting front can be exposed to changing power densities. This zone is followed in time by a brighter zone marking a local maximum gray value with the gray value increasing in the case of longer irradiation at the lower power level. Reshaping the cutting front toward a new steady state at the lower laser power puts it in a more favorable position for light absorption and thus increased heating when the laser power is increased back to the higher level, especially in the upper section. On the other hand, a too short reduction of the laser power does not yield a significant change of shape and position of the cutting front that generates overheating in the upper region with the increase of laser power capable of exceeding the already characteristic warmer lower region. The maximum displacement of the front during 0.1 ms at a cutting speed of 4 m/min is below 7 μm, which means that not much extra material has to be removed when the laser power is increased. Therefore, in this case, the characteristic peak after increasing the laser power is not prominent in the photodiode signals.

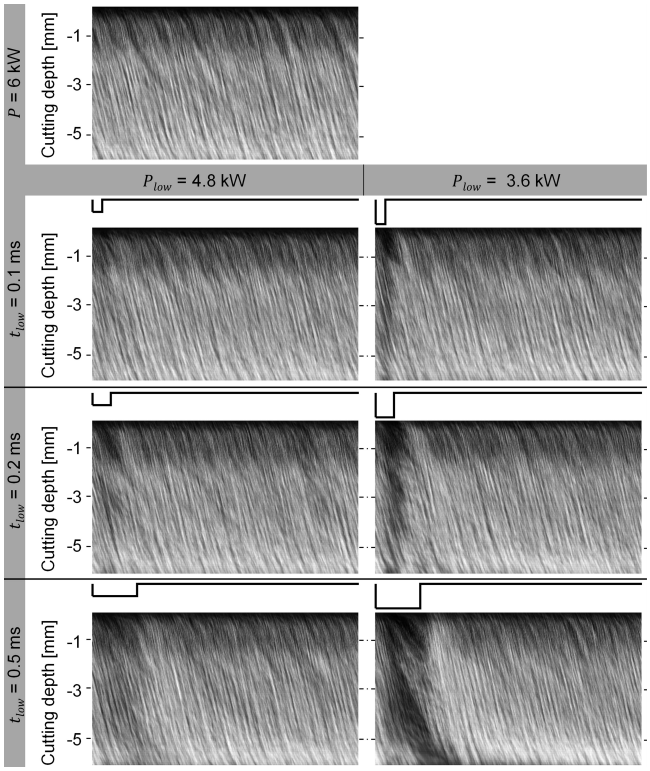

FIGURE 4 Overview of the streak images of the cutting front apex (averaged over 12 modulation periods resulting in an averaging time of t = 36 ms).

The process response to a reduction of the laser power to 3.6 kW is analyzed in more detail using an image sequence, Figure 5. The average gray value of different sections of the images, i.e., the entire image, the upper half, and the lower half, are calculated and compared with the VIS-signal. In the steady state right before the reduction of the laser power, smaller and darker melt waves can be seen in the upper third section, whereas they become larger and brighter further downstream, reflecting the higher temperature in the lower part of the cutting front. Reducing the laser power from 6.0 kW to 3.6 kW lasts 0.1 ms, and simultaneously the temperature on the entire cutting front is proportionally reduced to the minimum level. The shape and position of the cutting front with respect to the laser beam axis are affected

15214052, 2024, 1, Downloaded from https://onlinelibrary.wiley.com/doi/10.1002/mawe.202300141 by Rwth Aachen Hochschulbibliothek, Wiley Online Library on [15/05/2024]. See the Terms and Conditions (https://onlinelibrary.wiley.com/terms-and-conditions) on Wiley Online Library for rules of use; OA articles are governed by the applicable Creative Commons License

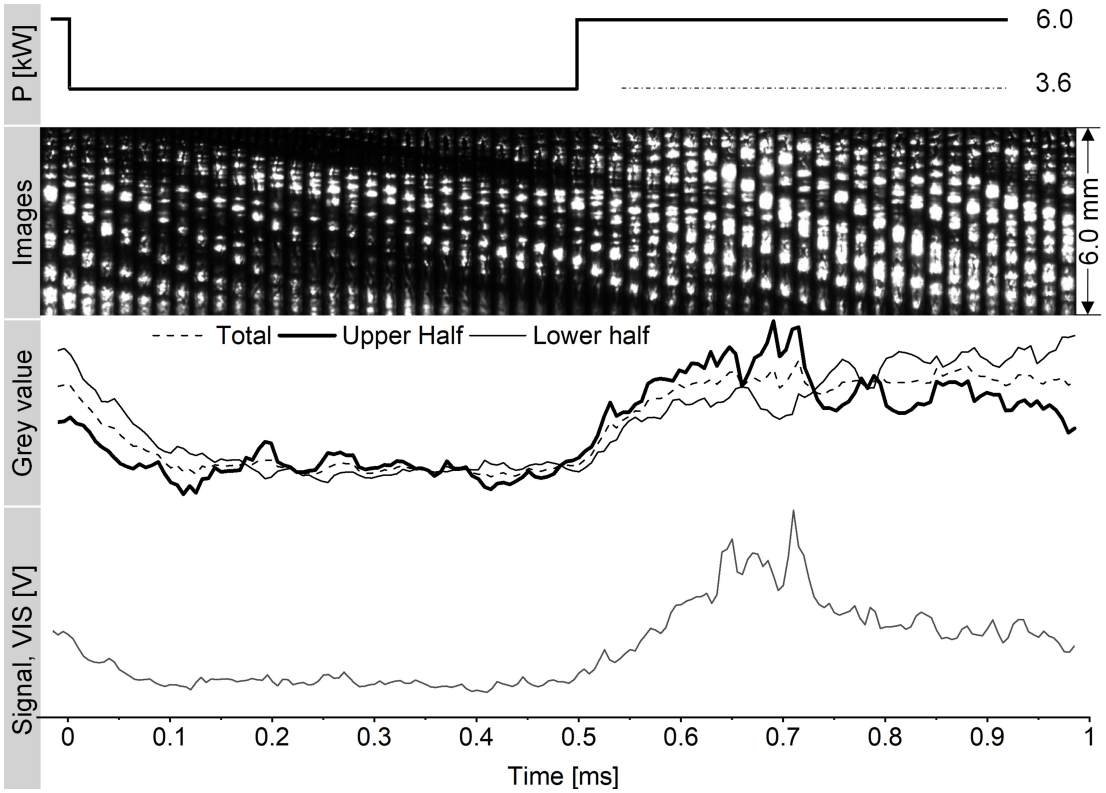

FIGURE 5 Correlation between nominal laser power, average gray value in the high-speed images and photodiode signal in visible range; sequence of images with interval of 18.43 µs. (Parameters: $P_{low} = 3.6$ kW; $t_{low} = 0.5$ ms)

by that [7,8]. First, the cutting front is shifted towards the laser beam axis, resulting in a flatter profile at the very top and a steeper profile on most of the cutting front. The steeper profile reduces the angle of incidence of the laser beam on the cutting front, which, in conjunction with the typical melt accumulations that form in the melt stream, increases the portion without direct laser radiation creating a "shadowing" effect, especially below the melt accumulations. The adaptation of the cutting front geometry to fulfil the power balance leads to a relaxation movement and the shadowing gradually decreases. The heating of the cutting front when the laser power is increased to 6 kW naturally leads to a reversal effect shifting the cutting front further away from the laser beam axis in the cutting direction. The average temperature at the cutting front increases immediately with the laser power and reaches an intermediate level in about 0.1 ms. Still, the local temperature of the upper section of the front continues to rise to a maximum for another 0.1 ms, and after reaching the highest temperature, it takes about additional 0.2 ms to reach a steady state again.

Further, it is investigated whether a short and moderate reduction of the laser power affect the quality of the cut flanks using 3D images. The produced cut flanks are generally characterized by three predominant zones, Figure 6 (left-hand side). The color indicates the height, which visualizes the flank profile from top to bottom and the striation pattern along the cut. Particularly in the upper third, the cut flanks have a concave profile with fine, regular striations. Shortly above the middle of the cut depth, the height reaches the maximum, i.e., the narrowest point of the kerf. The striations are tilted backwards, and the wavelength of the striations increases. The kerf is locally widened in the lowest third, indicated by the green areas. The average surface roughness R_z was measured in each of the three predominant zones at an interval of 1.5 mm, Figure 6 (right-hand side). The measured R_z values of the cuts produced by minimally invasive laser modulation deviate in both directions less than 15% from the reference cut, many of them being even lower than those of the reference cut. Furthermore, the cut flank with the highest R_z value (i.e., $P_{low} = 4.8$ kW and $t_{low} = 0.2$ ms) is compared with the reference cut in the exact section where the roughness measurement was carried out, Figure 6. Although the cut flank with this laser modulation parameter has a higher R_z value, the striation pattern profile revealed by the 3D images is nearly identical, implying that the difference in R_z does not indicate a modulation effect.

15214052, 2024, 1, Downloaded from https://onlinelibrary.wiley.com/doi/10.1002/mawe.202300141 by Rwth Aachen Hochschulbibliothek, Wiley Online Library on [15/05/2024]. See the Terms and Conditions (https://onlinelibrary.wiley.com/terms-and-conditions) on Wiley Online Library for rules of use; OA articles are governed by the applicable Creative Commons License

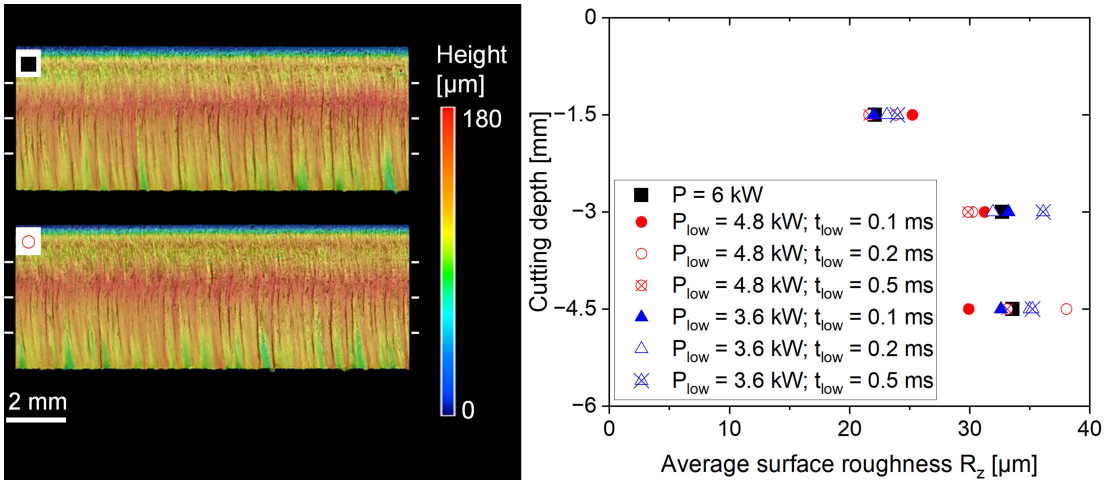

FIGURE 6 Left: R_z value as function of cutting depth for all investigated parameters; Right: 3D images of the cut flanks. (Reference cut and P_{low} = 4.8 kW, t_{low} = 0.2 ms)

6 | SUMMARY AND OUTLOOK

Minimally invasive laser modulation provides characteristic response signals being utilizable for real-time process state identification in laser cutting for process control applications. High-speed videography was employed to provide a spatially and temporally resolved, in-depth analysis of the process response to the laser power modulation on the cutting front. The variation in thermal radiation and geometry of the cutting front under short and moderate reduction of the laser power was analyzed and discussed.

It is concluded that the reduction of the laser power to 4.8 kW, i.e., to 80% of the maximum laser power, is not sufficient for inducing a characteristic process response at a sheet thickness of 6 mm in the stable working condition at a speed of 80% of the cutting speed limit. A sufficient impact on the process response is obtained by the reduction of the laser power to 3.6 kW, i.e., to 60% of the maximum laser power. In general, the reduction of the laser power leads to an instantaneous temperature decrease of the melt film surface. The reduction of the laser power with a duration of 0.5 ms causes a significant process response based on a flattening of the cutting front and its prolonged shift in the direction of the laser beam axis. Once the laser power is increased again, more material must be melted and removed to reshape the cutting front back to the original steady state, compared to the cases with shorter duration of the laser power at the lower level. After the laser power has reached the higher level, especially the temperature of the upper part of the front continues to rise to the maximum temperature for about 0.1 ms, resulting in the characteristic peak in the photodiode signals. Furthermore, it was demonstrated that minimally invasive laser modulation does not compromise the quality of the cutting flanks in the stable working condition at a speed of 80% of the cutting speed limit.

The results presented here provide the foundation for further investigations to extend the application range of a monitoring system based on minimally invasive laser modulation for thicker sheets. In this regard, the alteration of the features in the response signals as a function of critical process parameters such as cutting speed and focus position will be analyzed to allow, on this basis, the prediction of the reach to the cutting limit, which is a key factor for optimizing cutting efficiency and cut flank quality.

ACKNOWLEDGEMENTS

The presented investigations were carried out at the Chair of Laser Technology LLT of RWTH Aachen University and Fraunhofer Institute for Laser Technology ILT within the framework of the collaborative Research Centre SFB1120-236616214 “Bauteilpräzision durch Beherrschung von Schmelze und Erstarrung in Produktionsprozessen” and funded by the Deutsche Forschungsgemeinschaft e.V. (DFG, German Research Foundation). The sponsorship and support are gratefully acknowledged. Open access funding enabled and organized by Projekt DEAL.

REFERENCES

1. D. Belforte, *PhotonicsViews* **2020**, *2*, 35.
2. L. D. Scintilla, L. Tricarico, A. Mahrle, A. Wetzig, T. Himmer, E. Beyer, presented at *ICALEO’10*, Anaheim, CA, USA, **2010**, pp. 249–258.
3. M. Hansmann, I. A. Decker, J. L. Ruge, presented at the *International Conference on Power Beam Technology*, Brighton, 10–12 September, 1986, pp. 440–445.

15214052, 2024, 1, Downloaded from https://onlinelibrary.wiley.com/doi/10.1002/mawe.202300141 by Rwth Aachen Hochschulbibliothek, Wiley Online Library on [15/05/2024]. See the Terms and Conditions (https://onlinelibrary.wiley.com/terms-and-conditions) on Wiley Online Library for rules of use; OA articles are governed by the applicable Creative Commons License

4. F. Olsen, K. E. Andersen, N. Raben, F. B. Thomassen, presented at *LAMP'87*, Osaka, Japan, May, 1987, pp. 267–272.
5. M. Schleier, B. Adelmann, B. Neumeier, R. Hellmann, *Optics and Laser Technology* **2017**, *96*, 13.
6. N. Levichev, G. C. Rodrigues, J. R. Duflou, *Procedia CIRP* **2020**, *94*, 499.
7. H. Zefferer, Hartmut, *Ph.D. Thesis*, RWTH Aachen, Germany, **1998**.
8. H. Zefferer, D. Petring, W. Schultz, F. Schneider, G. Herziger, presented at *LASER'93*, Munich, Germany, **1993**.
9. F. Schneider, D. Petring, R. Poprawe, presented at *LIM'05*, Munich, Germany, 13–16 June, 2005.
10. D. Arntz, D. Petring, S. Stoyanov, U. Jansen, F. Schneider, R. Poprawe, *J. Laser Appl.* **2018**, *30*, 032206.
11. D. Arntz, D. Petring, F. Schneider, R. Poprawe, *J. Laser Appl.* **2019**, *31*, 032206.

How to cite this article: M. de Oliveira Lopes, F. Schneider, D. Petring, A. Gillner, *Materialwiss. Werkstofftech.* **2024**, *55*, e202300141.
https://doi.org/10.1002/mawe.202300141

15214052, 2024, 1, Downloaded from https://onlinelibrary.wiley.com/doi/10.1002/mawe.202300141 by Rwth Aachen Hochschulbibliothek, Wiley Online Library on [15/05/2024]. See the Terms and Conditions (https://onlinelibrary.wiley.com/terms-and-conditions) on Wiley Online Library for rules of use; OA articles are governed by the applicable Creative Commons License